International Journal of Automotive Technology, Vol. 5, No. 4, pp. 287–295 (2004)

1229-9138/2004/018-07

DEVELOPMENT OF FUEL CELL HYBRID ELECTRIC VEHICLE PERFORMANCE SIMULATOR

C. PARK, K. OH, D. KIM and H. KIM*

School of Mechanical Engineering, Sungkyunkwan University, Gyeonggi 440-746, Korea

(Received 5 September 2003; Revised 21 February 2004)

ABSTRACT–A performance simulator for the fuel cell hybrid electric vehicle (FCHEV) is developed to evaluate the potentials of hybridization for fuel cell electric vehicle. Dynamic models of FCHEV's electric powertrain components such as fuel cell stack, battery, traction motor, DC/DC converter, etc. are obtained by modular approach using MATLAB SIMULINK. In addition, a thermodynamic model of the fuel cell is introduced using bondgraph to investigate the temperature effect on the vehicle performance. It is found from the simulation results that the hybridization of fuel cell electric vehicle (FCEV) provides better hydrogen fuel economy especially in the city driving owing to the braking energy recuperation and relatively high efficiency operation of the fuel cell. It is also found from the thermodynamic simulation of the FCEV that the fuel economy and acceleration performance are affected by the temperature due to the relatively low efficiency and reduced output power of the fuel cell stack at low temperature.

KEY WORDS : Fuel cell hybrid electric vehicle, Proton exchange membrane, Operation algorithm, Regenerative braking

1. INTRODUCTION

Growing concerns on CO_2 reduction and limited energy source have been demanding cleaner and more energy efficient vehicle without compromising any convenient features of the conventional internal combustion engine vehicles. To meet such demands, automotive manufacturers have investigated alternative drivetrains such as H_2/CNG driven engine, electric vehicles (EV), hybrid electric vehicles (HEV) and fuel cell electric vehicles. In a comparison of these alternate drivetrains, they show advantages and disadvantages at different criteria. Vehicle manufacturers claim that FCEVs are very promising in long term base in terms of performance, efficiency and compliance with emission reduction schedules (Yang, 2000).

Basically, a fuel cell vehicle uses a fuel cell stack instead of a battery as the major source of electric power to drive an electric traction motor. The simplest configuration is supplying hydrogen directly from a hydrogen tank stored as a compressed gas or cryogenic liquid. FCEV can give a driving range comparable to an IC engine vehicle because its driving range is determined only by the amount of fuel available in the fuel tank (Chan, 2002). The key in development of FCEV is to offer the same package of performance and price as conventional drives. In recent years, major automotive manufacturers have developed and introduced several prototype FCEVs with various fuel options. Although there is a major issue with the hydrogen supply infrastructure, these prototype FCEVs have been demonstrating various favorable features of FCEVs as well as providing the guidelines for the future development directions. In addition, the recent technological advances in the proton exchange membrane (PEM) fuel cells have been showing promising results for transportation applications complementing the drawbacks of battery technologies.

Conventional fuel cell vehicles only use the fuel cell power for the vehicle propulsion. Hence the vehicle has no regenerative energy recovery in braking, and a long start-up time, and poor transient response with complex fuel cell and auxiliary system management. These shortcomings can be overcome by hybridization of FCEV using batteries. It is expected that FCHEVs can offer faster transient response at start, the energy recuperation capability in the regenerative braking and more efficient system operation by adequate operation algorithm, etc. However, such potentials for hybridization should be validated by considering the added weight and complexity (Friedman, 1999). In order to explore the potential improvement of the hybridization and evaluate different components or layout, and to predict the dynamic behavior, a dynamic simulator based on the FCHEVs powertrain model is required. In addition, to operate FCHEV, an appropriate operating algorithm is required. For instance, power distribution ratio between the fuel

*Corresponding author. e-mail: hskim@me.skku.ac.kr

cell and the battery should be provided for a given driver's demand and vehicle driving conditions (Paganelli, 2002).

A PEM fuel cell's voltage-current characteristics and efficiency are dependent on temperature (Gurski, 2003). These fuel cell system temperature property impacts not only vehicle fuel economy, but also performance such as acceleration and driveablility. Thus, it is important to know how the fuel cell system thermal property affects the fuel economy and driveability of a fuel cell vehicle.

In this paper, first the potential for hybridization of FCEV is investigated from the viewpoint of overall efficiency of the fuel cell system by considering the benefit of regenerative braking and the added weight. A FCHEV performance simulator is developed using MATLAB SIMULINK. In addition, operation algorithm how to distribute the required vehicle power to the fuel cell stack and the battery is proposed and evaluated by the simulator. Second, to understand the impact of temperature on vehicle performance better, simulation is performed initially started at 20°C (cold) and 80°C (hot). Also a full power acceleration 0 to 100 KPH is performed to evaluate vehicle acceleration performance.

2. FCHEV'S POWERTRAIN MODELING

Figure 1 shows a structure of the FCHEV used in this study. The FCHEV used in this study consists of proton exchange membrane type fuel cells, induction motor and 6.5Ah Ni-MH battery system. The traction motor is connected by a 10.03:1 reduction gear to the wheel of vehicle. The DC/DC converter between the fuel cell stack and battery allows the fuel cell system to operate at a steady state independent of the battery voltage and of the electric load imposed by the drivetrain and auxiliaries. Compressed hydrogen is supplied directly to the fuel cell stack. The FCHEV used in this study adopts a front-wheel drive.

2.1. Fuel Cell Stack

The PEM fuel cell stack consists of 280 cells and is capable to produce maximum of 75 kW. Performances of fuel cells are affected by the membrane, electrode, cell

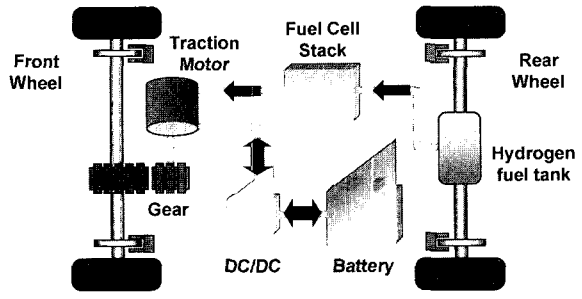

Figure 1. Structure of fuel cell hybrid electric vehicle.

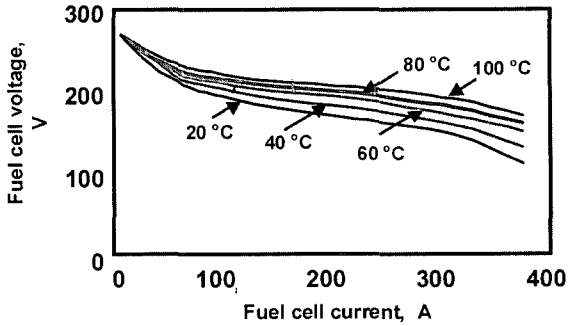

(a) Voltage-current characteristic curve

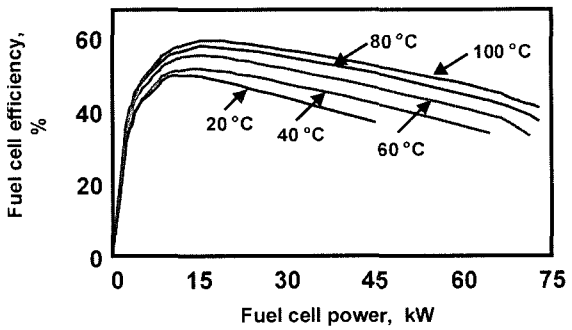

(b) Fuel cell system power and efficiency

Figure 2. Characteristics of fuel cell stack.

design, stack temperature, inlet pressure of hydrogen and oxygen. In this study, it is assumed that the pressure is constant at atmospheric pressure.

The stack voltage is defined as the sum of three terms, namely activation polarization, ohmic polarization and concentration polarization (Larminie, 2000). The relationship of current and voltage is expressed in the following equations and shown in Figure 2(a).

$$V(t)_{cell} = N_{cell} \times (E_{cell} - V_{activation} - V_{ohmic} - V_{concentration}) \quad (1)$$

$$E_{cell} = -\frac{\Delta g}{ZF} + \frac{RT}{ZF}\ln\left(\frac{P_{H_2} P^{1/2}{}_{O_2}}{P_{H_2O}}\right) \quad (2)$$

$$V_{activation} = \frac{RT}{2\alpha F}\ln\left(\frac{i_n + i(t)}{i_o}\right) \quad (3)$$

$$V_{ohmic} = (i_n + i(t)) \times r \quad (4)$$

$$V_{concentration} = \frac{RT}{ZF} ln\left(1 - \frac{i_n + i(t)}{i_l}\right) \quad (5)$$

where $V(t)_{cells}$ is the stack voltage, N_{cell} is the number of cells in stack, E_{cell} is the open circuit voltage, $V_{activation}$ is the activation polarization, $V_{concentration}$ is the ohmic polarization, is the concentration polarization, Δg is the Gibbs free energy, Z is the number of electron, is the Faraday constant (96485 coulomb), R is the gas constant, T is the operation temperature, P_{H_2}, $P^{1/2}{}_{O_2}$, P_{H_2O} is the partial pressure, α is the charge transfer coefficient, i_n is the

internal and fuel crossover equivalent current density, i_o is the exchange current density, r is the stack internal resistance, i_l is the limit current density.

The fuel cell system efficiency, including the energy consumption of auxiliary parts, such as the air compressor, fuel pump, water pump is shown in Figure 2(b). The amount of hydrogen flowing to the respective electrodes is related to the current i generated by the fuel cell stack.

$$mn_2 = 2.02 \times 10^{-3} \times \frac{1}{2F} \times i(t) \times N_{cell}[kg/s] \quad (6)$$

The actual amount of hydrogen usage can be obtained by considering the fuel cell stack efficiency shown in Figure 2(b).

2.2. Traction Motor

In Figure 3, a motor characteristic map used in the modeling is shown. The traction motor output torque is determined as the smaller torque by comparing the target motor torque which is calculated from the controller by drivers intention and the maximum motor torque available at the present motor speed and present system voltage. The maximum motor torque can be determined from Figure 3 depending on the voltage and motor speed (Hauer, 2000). The desired motor current $i_{desired}$ to generate output torque T_m is expressed as

$$i_{desired} = \frac{T_m \times \omega_m}{V_{bus} \times \eta_{motor}} \quad (7)$$

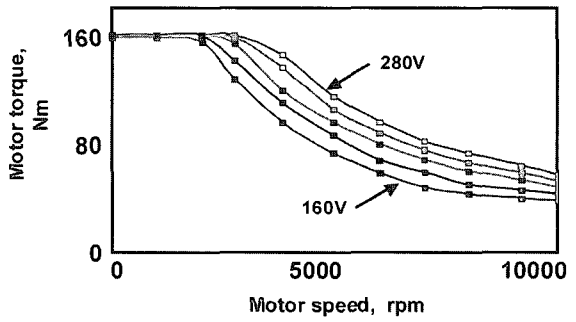

(a) Motor characteristic map

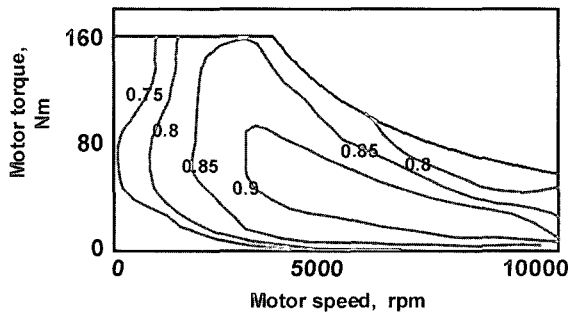

(b) Motor efficiency map

Figure 3. Characteristics of induction motor.

where V_{bus} is the system voltage, η_{motor} is the motor efficiency.

In regenerative braking, the motor is in generator mode and the same motor map with negative torque and positive speed can be used.

2.3. Battery

The input and output current of the battery and the SOC are calculated using the battery internal resistance model. The internal resistance is obtained from the experiments with respect to the battery SOCs. The battery voltage is represented as

$$U_a = E - i_a R_i \text{ at discharge} \quad (8)$$

$$U_a = E + i_a R_i \text{ at charge} \quad (9)$$

where U_a is the battery voltage, E is the electromotive force, i_a is the battery current, R_i is the internal resistance.

The battery power is expressed as a function of voltage and current.

$$P_{battery} = E \times i_a - i_a^2 R_i \quad (10)$$

The battery current at discharge can be obtained from the electromotive force, internal resistance and battery power required to drive the motor as

$$i_{battery\ discha\ arge} = \frac{E - \sqrt{E^2 - 4R_i P_{battery}}}{2R_i} \quad (11)$$

The battery current at charge can be obtained in similar fashion. The battery SOC is directly related with the battery capacity

$$Q_u(i_a, t, \tau) = Q_\tau(i_a, t) - \int_0^t i_a(t)dt \quad (12)$$

where Q_u is the temporary usable capacity which is a function of the current i_a, temperature t, and time τ, Q_τ is the accumulators capacity. The integral term in Equation (12) is the usable charge, which has been drawn from the accumulator.

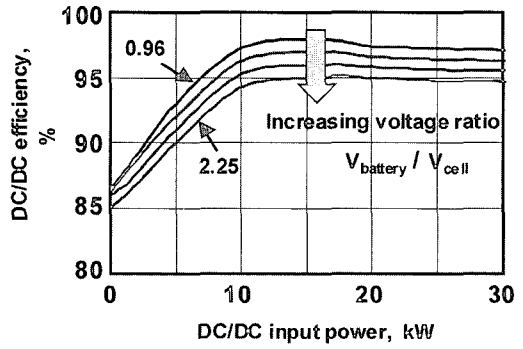

Figure 4. DC/DC converter sinking and sourcing efficiency variation with voltage ratio.

2.4. DC/DC Converter

The DC/DC converter decouples the battery voltage from the system voltage and allows the fuel cell system to operate at a steady state independent from the battery voltage (Goodarzi, 2002). The efficiency of the DC/DC converter when sourcing and sinking depends on the power and voltage ratio. In Figure 4, a DC/DC converter efficiency is shown.

2.5. Vehicle

The FCHEV vehicle dynamics is expressed as

$$\frac{dV}{dt} = \frac{\frac{N_f}{R_t}T_m - F_L - F_b}{M + \left(J_m + J_g + \frac{2J_t}{N_f^2}\right)\frac{N_f^2}{R_t^2}} \tag{13}$$

where N_f is the reduction gear ratio, R_t is the tire radius, T_m is the motor torque, F_L is the road load, F_b is the braking force, M is the vehicle mass, J_m is the motor inertia, J_g is the gear and shaft inertia and J_t is the wheel inertia.

3. THERMODYNAMIC MODELING OF FUEL CELL STACK

The voltage-current characteristics and efficiency of the fuel cell depend on the temperature. In the fuel cell process, a half of the hydrogen energy is used to generate the electric energy and the remaining energy is transformed into the heat. The heat generated in the stack is presented

$$\begin{aligned} Q(t) &= N_{cell} \times i(t) \times (E_{cell} - V(t)_{cell}) \\ &= P(t)_{cell} \times \left(\frac{E_{cell}}{V(t)_{cell}} - 1\right) \end{aligned} \tag{14}$$

where N_{cell} is the number of the cell, $C(t)_{cell}$ is the stack output voltage, $P(t)_{cell}$ is the output power, E_{cell} is the open circuit voltage of the fuel cell.

In Figure 5, structure of unit fuel cell is shown. The membrane electrode assembly (MEA) which consists of the electrolyte, cathode and anode is combined with two bipolar plates to form one unit cell. The heat generated in the MEA is transmitted to the bipolar plates and the temperature of the bipolar plates is controlled by the coolant and convective heat of the reaction fluids.

In this study, it is assumed that the fuel cell temperature is represented by the bipolar plate temperature. Bondgraph for thermodynamic model of a unit fuel cell is shown in Figure 6. It is seen from Figure 6 that $Q(t)$ that is generated in the fuel cell is converted to the rate change of the entropy through the R-field. In the bipolar plates, heat convection occurs through the hydrogen, air and coolant, which is modeled as R-field.

From the bondgraph, the rate change of the fuel cell entropy S_{cell} is obtained

$$\dot{S}_{cell} = \dot{S}_{input} - \dot{S}_{H_2} - \dot{S}_{air} - \dot{S}_{coolant} \tag{15}$$

where $\dot{S}_{input}$ is the rate change of the entropy due to the heat generated in the cell, $\dot{S}_{H_2}$ is the rate change of the hydrogen entropy, $\dot{S}_{air}$ is the rate change of the air entropy and $\dot{S}_{coolant}$ is the rate change of the coolant entropy.

The heat convected by the hydrogen Q_{H_2} is represented

$$Q_{H_2} = h_{H_2} \times A_{vent}(T - T_{H_2}) \tag{16}$$

where h_{H_2} is the convection coefficient, A_{cent} is the convection area, T is the fuel cell temperature, T_{H_2} is the hydrogen inlet temperature. The heat convected by the air and the coolant can be obtained in a similar manner. From the heat ΔQ balance, the heat to increase the fuel cell can be represented

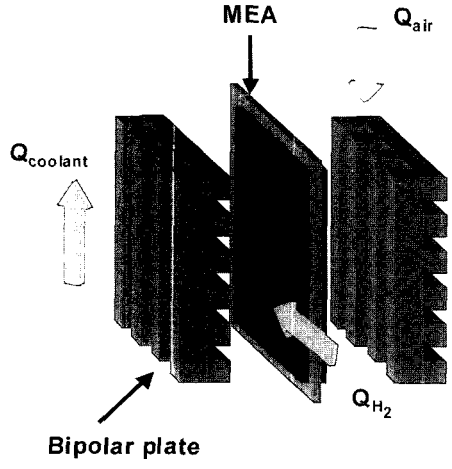

Figure 5. Structure of a unit cell.

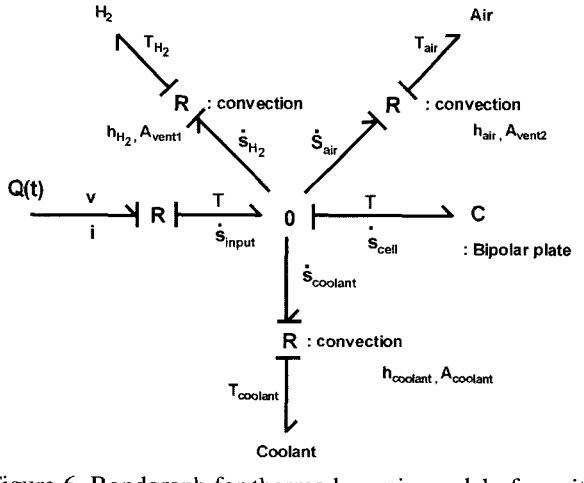

Figure 6. Bondgraph for thermodynamic model of a unit cell.

$$\Delta Q = Q(t) - Q_{H_2} - Q_{air} - Q_{coolant} = m_{cell} \times C_p \times \Delta T \tag{17}$$

where m_{cell} is the mass of the bipolar plate, C_p is the specific heat. The rate change of the entropy is related with ΔQ as

$$\dot{S} = \frac{\Delta Q}{T} \tag{18}$$

From Equations (17) and (18), the temperature of the fuel cell can be obtained as

$$T(t)_{cell} = T(0)_{cell} \times \exp\left(\frac{S_{cell} - S_0}{m_{cell} \times C_p}\right) \tag{19}$$

where $T(0)_{cell}$ is the initial temperature.

4. FCHEV SIMULATOR

In Figure 7, a block diagram for FCHEV in normal driving mode is shown.

The driver operates the accelerator pedal corresponding to the velocity error between the target vehicle velocity and actual velocity. From the accelerator pedal position A_p, the drive power can be determined. The desired motor current $i_{desired}$ is obtained from the motor characteristic map by considering the motor efficiency. The drive power is delivered from two power sources: (1) fuel cell stack and (2) battery. The power distribution between the fuel cell stack and the battery is determined from the operation strategy to drive the vehicle.

In Figure 8, a block diagram for FCHEV in deceleration driving mode is shown. From the brake pedal position B_p, the braking force can be determined. Considering the battery SOC, brake pedal position, system voltage and vehicle velocity, BCU (brake control unit) determines the amount of friction braking and regenerative braking. If the demanded braking force is less than the regenerative braking force, only the regenerative braking is applied. In case that the demanded braking force is larger than the

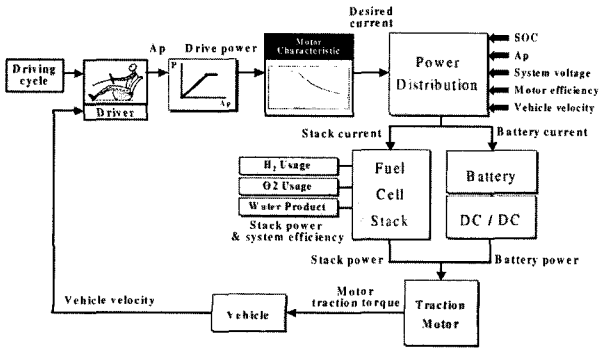

Figure 7. Block diagram for FCHEV in normal driving mode.

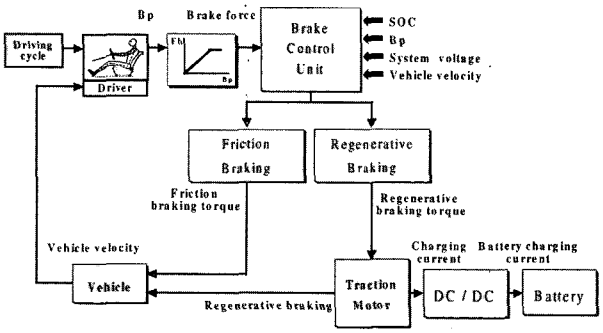

Figure 8. Block diagram for FCHEV in deceleration driving mode.

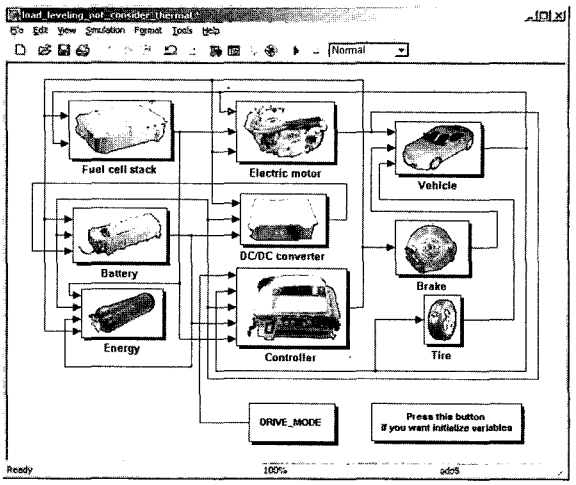

Figure 9. FCHEV performance simulator.

regenerative braking, the friction braking works together with the regenerative braking. In a regenerative braking, the motor is used as a generator and braking energy of the vehicle is stored in the battery.

Figure 9 shows the FCHEV performance simulator developed using MATLAB SIMULINK. The simulator consists of the fuel cell stack, battery, motor, DC/DC converter, vehicle, brake and tire module. Each module is constructed based on the dynamic model obtained.

5. FCHEV OPERATION ALGORITHM

For the FCHEV used in this study, power assist algorithm is proposed. In the power assist algorithm, the battery is used to assist the fuel cell while the fuel cell propels the vehicle as a primary power source. Also battery management strategy is applied to maintain the battery SOC. 5 operation modes are used; starting mode, constant mode, acceleration mode, deceleration mode and fuel cell-off mode (Oh, 2003). In actual driving, the FCHEV controller selects the appropriate operation mode from the signals such as the drivers intention and vehicle driving conditions.

Brief explanation of each operation mode is described as follows.

5.1. Starting Mode

In this mode, the vehicle starts only by the battery because the battery shows better response than the fuel cell stack in starting. However, battery drive can be applied only when the battery SOC and the required power meet pre-determined condition. For instance, if the battery SOC becomes lower than the bottom limit, the battery is switched off and the fuel cell stack is used to start the vehicle. The battery power is determined according to the following equation

$$P_{battery} = W_1(SOC) \times W_2(V) \times P_{peak} \quad (20)$$

where W_1 is the weight factor which is a function of the battery SOC, W_2 is the weight factor which is a function of the vehicle velocity, P_{peak} is the battery peak power. The battery discharge can be managed by Equation (20), which maintains the SOC above the bottom limit. In addition, if the demanded vehicle drive power is higher than the battery peak power, the fuel cell stack is also used together with the battery to propel the vehicle.

5.2. Constant Mode

This mode is applied when the vehicle runs at constant speed or mild acceleration. If the battery SOC is high enough and demanded vehicle power is small, vehicle is propelled only by the battery since the fuel cell stack efficiency is poor in the low power region. If demanded vehicle power is medium, vehicle is propelled only by the fuel cell stack since the stack efficiency is relatively high in the medium power region. When the battery SOC is low, the FCHEV is driven only by the fuel cell stack.

5.3. Acceleration Mode

This mode is applied when the vehicle runs at rapid acceleration or demanded vehicle power is high. Both battery and fuel cell stack are used to meet the high power requirement of vehicle.

5.4. Deceleration Mode

This mode is applied when the driver pushes the brake pedal or lifts up the accelerator pedal. In this mode, the regenerative braking is involved. When regenerative braking, if the demanded braking torque is smaller than the regenerative braking torque available at a given motor speed, only the regenerative braking is performed. If the demanded braking torque is larger than the regenerative braking torque, the conventional friction braking works simultaneously. In regenerative braking, the regenerative braking torque T_{REGEN} is controlled by the following equation

$$T_{REGEN} = W_3(SOC) \times W_4(V) \times T_m \quad (21)$$

where W_3 and W_4 are the weight factors, T_m is the regenerative torque available at a given motor (generator) speed. Eg. (21) prevents the battery from overcharging and provides the driver a comfort feeling at low speed braking (Yeo, 2002).

5.5. Fuel Cell-off Mode

In this mode, the fuel cell stops to eliminate the unnecessary idling operation, which contributes to improve the hydrogen fuel economy.

Mode selection is carried out depending on the acceleration pedal position, brake pedal position, vehicle velocity and battery SOC. The fuel economy of the FCHEV depends on the operation algorithm. In this study, power assist algorithm (Oh, 2003) is used. In the power assist algorithm, the fuel cell stack is used as the primary power source while the battery assists the fuel cell stack.

6. SIMULATION RESULTS

6.1. Benefit of Hybridization

Simulations are performed for the FCEV and the FCHEV to evaluate the potentials of the hybridization of the FCEV. In Table 1, vehicle parameters used in the simulation are shown.

In Figure 10, simulation results of the FCEV are shown for FUDS. In the simulation, the initial battery SOC is assumed to be 70%. The vehicle velocity (a) follows closely the driving mode. It is noted from (b) that large amount of motor torque is required at start. Although fuel cell power (c) shows about 50 kW of peak power, average power is under 20 kW for most of the driving schedule. Since the fuel cell system does not work at idle, the fuel cell power remains zero when the vehicle stops. Hydrogen fuel economy (d) is calculated as 0.065 km/g.

In Figure 11, simulation results of the FCHEV are

Table 1. Vehicle data.

Fuel cell stack (PEM)	Maximum power	75 kW
	Fuel type	Hydrogen
	Number of cell	280
Motor (AC)	Peak power	60 kW
	Rated speed	3600 rpm
	Maximum torque	160 Nm
Battery (Ni-MH)	Capacity	6.5 Ah, 40 module
Vehicle	Mass	FCEV : 1850 kg F900 kg
	Tire radius	0.343 m
	Frojection area	2.39 m^2
	Reduction gear ratio	10.03 : 1

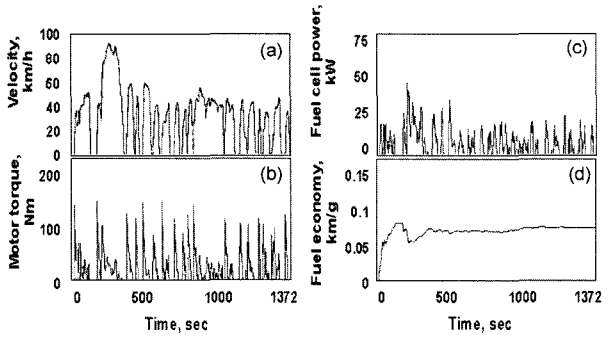

Figure 10. Simulator results of FCEV for FUDS.

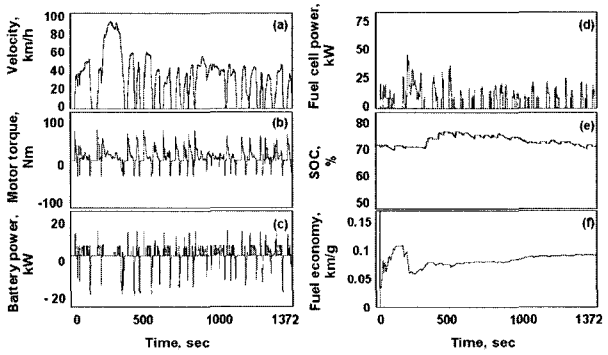

Figure 11. Simulator results of FCHEV for FUDS.

shown for FUDS. In the simulation, the power assist algorithm is applied. The vehicle velocity (a) follows closely the driving mode. The motor torque (b) shows a positive value when the motor is used to propel the vehicle and shows a negative value in the generator mode during the regenerative braking. Also the battery power (c) shows a positive value when the battery is used to propel the vehicle and shows a negative value during the regenerative braking.

For most of the driving mode, average battery power of less than 10 kW is used to assist the fuel cell. Due to the battery power assist, frequency and magnitude of the fuel cell power (d) decreases in comparison with those of the FCEV (Figure 10d). The fuel cell stack can be operated in relatively high efficiency region owing to the battery assist. The battery SOC (e) decreases from the initial SOC, in the starting, constant and acceleration mode meanwhile the SOC is increased by the regenerative braking in the deceleration mode. The battery SOC changes around the initial value, 70% due to the battery SOC management strategy. It is seen from (f) that the hydrogen fuel economy of the FCHEV is improved by 26% compared to that of the FCEV.

In Figure 12, the hydrogen fuel economies of the FCEV and FCHEV are compared for various driving cycles; FUDS, Highway and Japan 10–15 mode. For the

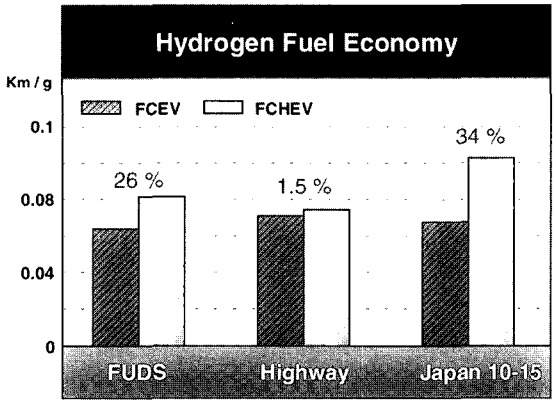

Figure 12. Comparison of hydrogen fuel economy for various driving cycles.

FCHEV simulation of each driving cycle, the final battery SOC is controlled to maintain the initial SOC within ± 0.5% by the battery SOC management strategy, which enables the comparison of the hydrogen fuel economy with that of the FCEV. It is seen from the simulation results that the hybridization of the FCEV provides 26% improvement of the fuel economy for FUDS and 34% improvement for Japan 10–15 mode. This improvement results from the recuperation energy in braking and operation of the fuel cell stack in relatively high efficiency region that will be explained in Figure 13. It is noted that the improvement percentage of the fuel economy is not much for Highway driving mode compared to those for city driving cycles since the recuperation energy in the Highway mode is not large enough to compensate the increased weight due to the hybridization.

Figure 13 shows efficiency of the fuel cell system for various driving cycles. The fuel cell system efficiency is obtained as an average value with respect to the required power during the driving cycle simulation.

As shown in Figure 13, the average fuel cell efficiency

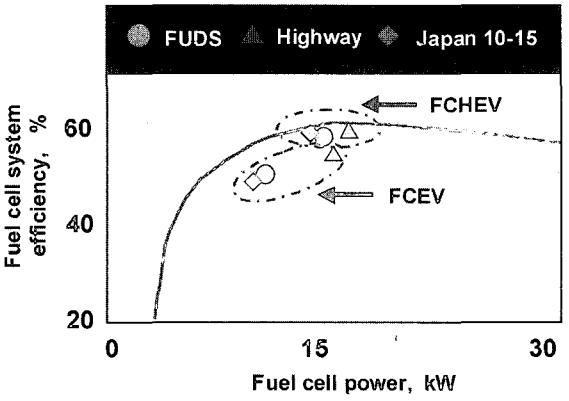

Figure 13. Average efficiency vs. power.

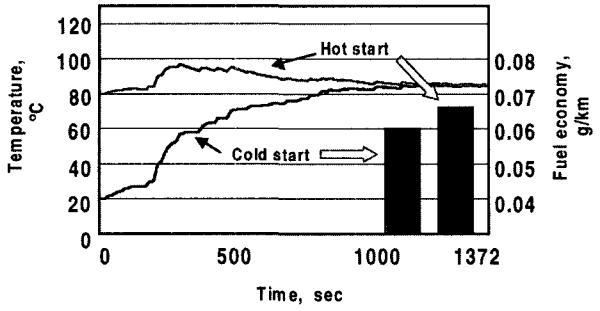

Figure 14. Comparison of temperature and hydrogen fuel economy for FUDS.

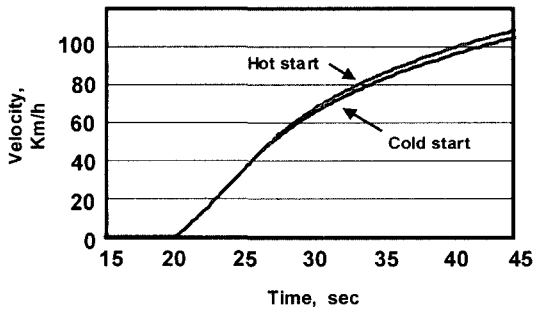

Figure 15. Cold and hot acceleration performance.

of the FCHEV moves to higher efficiency region by hybridization for FUDS and Japan 10–15 mode. This is because the average fuel cell power of the FCHEV increases for the small power by the battery operation and decreases for the large power by the battery assist. However, for the Highway mode, the improvement percentage by the hybridization is not much since the fuel cell system is operated in relatively high efficiency region without the battery assist. It is noted from Figure 13 that the potential advantage for hybridization of the FCEV can be achieved for city driving where frequent stop and go is expected.

6.2. Effect of Temperature on Vehicle Performance

To evaluate the temperature effect on the vehicle performance, simulations are performed for the cold and hot start conditions. For the cold start, the initial temperature $T(0)_{cell}$=20°C is used meanwhile $T(0)_{cell}$=80°C is used for the hot start simulation.

In Figure 14, the temperature responses are compared. It is seen from Figure 14 that a warming up time is required for the cold start until the fuel cell temperature reaches its steady state. During the warming up period, the fuel cell stack is operated in the relatively low efficiency region (Figure 2b), which results in the low fuel economy for the FUDS (Figure 14).

In Figure 15, the acceleration performance is compared. The 100 KPH reaching time at WOT for the cold start is 1.6 seconds longer than that of the hot start for the target vehicle. This is because the maximum output power is reduced due to the relatively large voltage drop when the fuel cell is operated in the low temperature.

7. CONCLUSION

A performance simulator for the FCHEV is developed to evaluate the potentials of hybridization for fuel cell electric vehicle. Dynamic models of FCHEVs electric powertrain components such as fuel cell stack, battery, traction motor, DC/DC converter, etc. are obtained by modular approach using MATLAB SIMULINK. In addition, a thermodynamic model of the fuel cell is introduced using bondgraph to investigate the temperature effect on the vehicle performance. It is found from the simulation results that the hybridization of FCEV provides better hydrogen fuel economy especially in the city driving owing to the braking energy recuperation and relatively high efficiency operation of the fuel cell. It is also found from the thermodynamic simulation of the FCEV that the fuel economy and acceleration performance are affected by the temperature due to the relatively low efficiency and reduced output power of the fuel cell stack at low temperature.

ACKNOWLEDGEMENT–The authors wish to thank for the support by Brain Korea 21 Project in 2003 and Fuel Cell Vehicle Team in Hyundai Motor Company.

REFERENCES

Chan, C. C., Wong, Y. S. and Chau, K. T. (2002). Optimal design of hybrid fuel cell electric vehicle. *19th Electric Vehicle Symposium.*

Friedman, D. J. (1999). Maximizing direct hydrogen PEM fuel cell vehicle efficiency Is hybridization necessary?. *SAE Paper No.* 1999-01-0530.

Goodarzi, G. A. and Yum, L. (2002). Fuel cell system architecture. *19th Electric Vehicle Symposium.*

Gurski, S. D. and Nelson, D. J. (2003) Cold start fuel economy and power limitations for a PEM fuel cell vehicle. *SAE Paper No.* 2003-01-0422.

Hauer, K. H., Moore, R. M. and Ramaswamy, S. (2000). The hybridized fuel cell vehicle model of the university of California. Davis, *SAE Paper No.* 2001-01-0543.

Larminie, J. and Dicks, A. (2000). *Fuel Cell Systems Explained.* John Wiley & Sons, Ltd. West Sussex.

Oh, K. C. and Kim, H. S. (2004). Operation algorithm for a parallel hybrid electric vehicle with a relatively small electric motor. *KSME Int. Journal* **18, 1,** 30–36.

Paganelli, G., Guezennec, Y. and Rizzoni, G. (2002).

Optimizing control strategy for hybrid fuel cell electric vehicle. *SAE Paper No.* 2002-01-0102.

Yang, W. C. (2000). Fuel cell electric vehicle: Recent advances and challenges. *Int. J. Automotive Technology* **1. 1.** 9–16.

Yeo, H., Kim, T. C., Kim, C. S. and Kim, H. S. (2002). Performance analysis of regenerative braking system for parallel hybrid electric vehicle using HILS. *19th Electric Vehicle Symposium.*